



# Journal of Applied Sciences

ISSN 1812-5654

**science**  
alert

**ANSI***net*  
an open access publisher  
<http://ansinet.com>

## Finite-Difference Time-Domain Method Solution of Fundamental Space-Filling Mode in Photonic Crystal Fibers

<sup>1</sup>M. Mansourabadi, <sup>1</sup>A. Poorkazemi, <sup>1</sup>M. Shamloufard and <sup>2</sup>Y. Riazi

<sup>1</sup>K.N. Toosi University of Technology, Faculty of Electrical Engineering, Seyedkhandan, Dr. Shariati Avenue, P.O. Box 16315-1355, Tehran, Islamic Republic of Iran

<sup>2</sup>K.N. Toosi University of Technology, Faculty of Science, No. 41, Kavian Street, Mojtabaie Street, Seyed Khandan Bridge, Shariyati Avenue, P.O. Box 16315-1618, Tehran, Islamic Republic of Iran

---

**Abstract:** In this study, a Finite-Difference Time-Domain (FDTD) method for the full-vectorial analysis of Fundamental Space-filling Mode (FSM) of photonic crystal fibers is introduced. In order to increase the accuracy of results obtained by this method, an initial field distribution is proposed and Padé approximation technique is applied. By comparing the effective index and chromatic dispersion results obtained by FDTD method and FDTD Effective Index Method (FDTD-EIM), the influence of the accuracy of the solution on the Effective Index Method (EIM) which is based on FDTD is also investigated.

**Key words:** Effective index method, dispersion, Padé approximation, conformal technique, initial field distribution

---

### INTRODUCTION

In recent years, Photonic Crystals Fibers (PCFs) have attracted much attention due to some extraordinary properties, such as wide single-mode wavelength range, unusual chromatic dispersion and high or low non-linearity (Saitoh and Koshiba, 2005). Because of these properties, PCFs have turned out to be practical in various optical fields, such as nonlinear optics (Ranka *et al.*, 2000; Bowden and Zheltikov, 2002), ultrafast science (Reeves *et al.*, 2003), optical metrology (Udem *et al.*, 2002), nonlinear spectroscopy (Konorov *et al.*, 2004) and microscopy (Paulsen *et al.*, 2003), biomedical optics (Hartl *et al.*, 2001) and optical sensing (Myaing *et al.*, 2003).

Index-guiding PCFs are usually formed by a central solid defect region surrounded by multiple air holes in a regular hexagonal array of wavelength-scale air holes running along the entire fiber length (Li *et al.*, 2004). Different modeling methods have been introduced to study the characteristics of PCFs, including the plane wave expansion method (Ferrando *et al.*, 1999), the Effective-Index Method (EIM) (Knight *et al.*, 1998), the Finite-Difference method in the Time Domain (FDTD) (Qiu, 2001) or Frequency Domain (FDFD) (Zhu and Brown, 2002) and the Finite Element Method (FEM) (Brecht *et al.*, 2000). Among these methods, the FDTD

method using Yee's mesh (Yee, 1966) has been successfully applied to PCFs and is much easier to implement while it can obtain comparable accuracy. A compact two-dimensional (2-D) scheme is usually used to compute guided modes in PCFs if one assumes that the propagation constant along the z-direction (propagation direction) is fixed (Qiu, 2001; Choi and Hoeffler, 1986; Asi and Shafai, 1992). Thus, it is possible to obtain the effective index ( $n_{\text{eff}}$ ) from PCF formed by a defect surrounded by circular air holes in hexagonal lattice.

The Fundamental Space-filling Mode (FSM) of a PCF is defined as the mode with the largest modal index of the infinite two-dimensional photonic crystal that constitutes the PCF cladding (Bjarklev *et al.*, 2003; Birks *et al.*, 1997). By solving FSM of a PCF, one can obtain the effective cladding index ( $n_{\text{FSM}}$ ).

Once having the effective cladding index and effective index, it is possible to calculate confinement loss (Koshiba and Saitoh, 2005), bending loss (Nielsen *et al.*, 2004), splice loss (Kliros *et al.*, 2006) and effective modal spot size (Kliros *et al.*, 2006) and to determine single-mode region (Birks *et al.*, 1997).

Also, in this study, an FDTD-based method for solving the FSM of PCFs is presented and the influence of the solution accuracy on the EIM is investigated by comparing  $n_{\text{eff}}$  and dispersion results obtained by FDTD and FDTD Effective Index Method (FDTD-EIM). To facilitate obtaining effective cladding index and the

effective index and to increase the accuracy of the algorithm, a specific initial field distribution is introduced and Padé approximation technique (Dey and Mittra, 1998) is introduced applied.

**NUMERICAL METHODS**

For a linear isotropic material in a source-free region, the time-dependent Maxwell's equations can be written as:

$$\nabla \times \vec{E} = -\mu(r) \frac{\partial \vec{H}}{\partial t} \tag{1}$$

$$\nabla \times \vec{H} = -\epsilon(r) \frac{\partial \vec{E}}{\partial t} + \sigma(r) \vec{E} \tag{2}$$

where,  $\mu(r)$ ,  $\epsilon(r)$  and  $\sigma(r)$  are the position-dependent permeability, permittivity and conductivity of the material, respectively.

According to Yee-cell technique, Maxwell's equations can be discretized in space and time on a discrete three-dimensional mesh (Qiu, 2001). Assuming that the fields of the guided modes in PCFs are dependent on  $\exp(j\beta_z z)$  ( $\beta_z$  is the propagation constant) along the propagation direction, the z-derivatives in Maxwell's equations can be replaced by  $j\beta_z$  and reexpressed in terms of the transverse variables only (Qiu, 2001).

To avoid introducing complex number into the computation, it is possible to assume that the TE field components ( $H_x, H_y, E_z$ ) are composed of the  $\cos(\beta_z z + \varphi)$  and the TM field components ( $E_x, E_y, H_z$ ) are composed of the  $\sin(\beta_z z + \varphi)$  contributions of complex exponential, so the resulting equations are faster and need less memory while the accuracy will remain the same (Qiu, 2001).

The algorithm stability is guaranteed as long as the time increment ( $\Delta t$ ) satisfies:

$$\Delta t \leq 1/c \sqrt{2\Delta h^{-2} + (\beta_z/2)^2}$$

where,  $c$  is the speed of the light and  $\Delta h = \Delta x = \Delta y$  is the dimension of unit cell of 2-D mesh (Qiu, 2001).

To solve a FSM problem, it is possible to apply Yee's algorithm to a unit cell that acts like a boundless propagation medium. Figure 1 shows the unit cell of cladding structure.

Considering the unit cell along with the Periodic Boundary Conditions (PBCs) expressed as Taflove and Hagness (2005):

$$\vec{E}_x \Big|_{i=0} = \vec{E}_x \Big|_{i=i_{max}} e^{j\beta_x L_x} \tag{3}$$

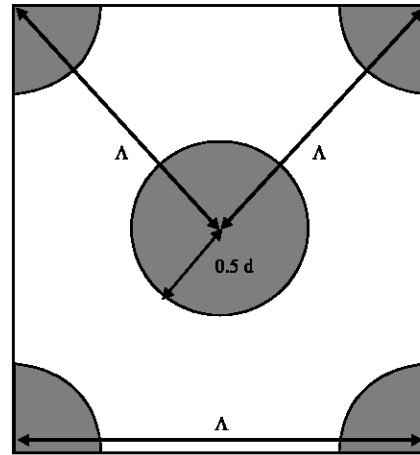


Fig. 1: The unit cell of cladding used to solve FSM problem

$$\vec{E}_x \Big|_{i=i_{max}+1} = \vec{E}_x \Big|_{i=1} e^{-j\beta_x L_x} \tag{4}$$

the unit cell can be set to act like 2-D infinite photonic crystal that constitutes the PCF cladding structure. Note that Eq. 3 and 4 are written along x-axis for  $E_x$  and other boundary conditions can be derived according to Taflove and Hagness (1995).

The 2-D photonic crystal unit cell of interest spans from FDTD grid cell  $(0, 0)$  and  $(0, j_{max})$  to  $(i_{max}, 0)$  and  $(i_{max}, j_{max})$ . On the other hand, the FDTD formulation (Qiu, 2001) is not able to calculate the x-component of electric fields at the first column grid points ( $i = 0, j$ ), thus it is enough to copy the fields at the last column grid points ( $i = i_{max}, j$ ) to those at the first column grid points according to Eq. 3. Since, it is merely interesting to calculate effective index of the infinite photonic crystal cladding, thus Eq. 3 can be reduced to:

$$E_x^n \Big|_{j=0} = E_x^n \Big|_{j=i_{max}} \tag{5}$$

which is definitely simpler and faster than Eq. 3 and 4. The following equations are obtained for the other field components in the same way.

$$E_y^n \Big|_{i=0} = E_y^n \Big|_{i=i_{max}} \tag{6a}$$

$$E_z^n \Big|_{i=0} = E_z^n \Big|_{i=i_{max}} \tag{6b}$$

$$E_z^n \Big|_{j=0} = E_z^n \Big|_{j=j_{max}} \tag{6c}$$

$$H_x^n \Big|_{j=i_{max}} = H_x^n \Big|_{j=0} \tag{7a}$$

$$H_y^n |_{i=i_{max}} = H_y^n |_{i=0} \quad (7b)$$

$$H_z^n |_{i=i_{max}} = H_z^n |_{i=0} \quad (7c)$$

$$H_z^n |_{j=j_{max}} = H_z^n |_{j=0} \quad (7d)$$

Note that Eq. 5 to 6c should be applied after electric fields calculation while (Eq. 7a-d) are applied after magnetic fields calculation.

To excite the structure, one can use point-wise source or artificial random initial field distribution (Taflove and Hagness, 1995; Qiu and He, 2000). However, by experience, it is found out that after the steady state is reached, the first mode will be dominant if initial field distribution introduced in the FDTD algorithm is approximately the same as field distribution of the first mode. This scheme has two important advantages in PCF simulations. First, it can reduce the needed total number of the time steps to reach steady state and second, the detection of the first mode is easier and more accurate. Assuming that the center of unit cell is located at  $(1/2i_{max}, 1/2j_{max})$ , it is practical to use the following relation to initialize x-component of electric field.

$$E_x^0 = \text{Exp}\left(\frac{i-0.5 \times i_{max}}{\alpha \times i_{max}}\right) \times \text{Exp}\left(\frac{j-0.5 \times j_{max}}{\beta \times j_{max}}\right) \quad (8)$$

By trial and error, the optimized value of 1.3 is found for  $\alpha$  and  $\beta$ . Figure 2 shows the results obtained by FFT from different excitations.

The accuracy of FFT results is dependent on the total number of time steps, which means a larger number of time

steps leads to more accurate result by FDTD. Thus, by using Padé approximation technique (FFT/Padé) reported by Dey and Mittra (1998), it is possible to efficiently increase the accuracy of FFT results obtained by simulation.

To verify the proposed method numerically, the fundamental space-filling mode formed by a hexagonal lattice of circular air holes in silica (Fig. 1) is studied. The lattice pitch is  $2.3 \mu\text{m}$  and the diameter of the air holes is  $d = 1 \mu\text{m}$ . Taking the time increment,

$$\Delta t = 0.1/c\sqrt{2\Delta h^{-2} + \beta_z^2} / 4$$

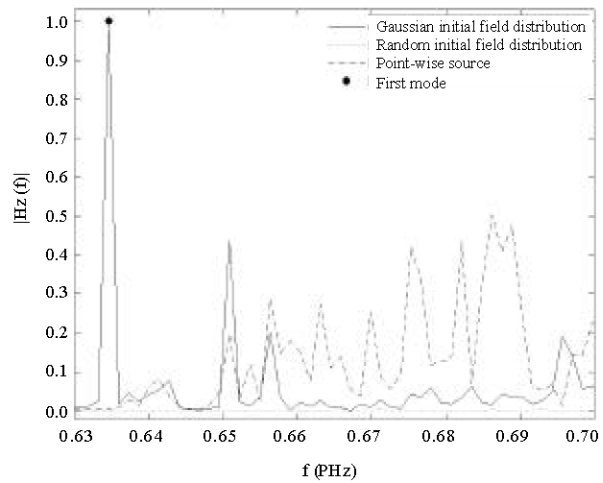


Fig. 2: FFT results by different excitations (Gaussian initial field distribution based on Eq. 8, random initial field distribution and point-wise source excitation) for  $\Delta h = 0.125 \mu\text{m}$ ,  $\Delta t = 1.246 \times 10^{-17} \text{sec}$ ,  $\beta_z = 1.9242 \times 10^7 \text{Rad m}^{-1}$ ,  $\Lambda = 2.5 \mu\text{m}$  and  $d/\Lambda = 0.3$

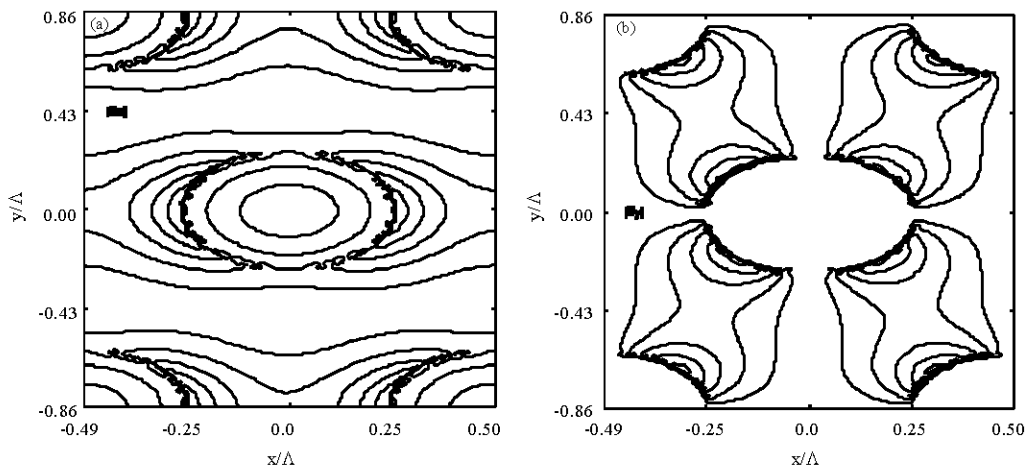


Fig. 3: Contour plots of the transverse electric-field components of the fundamental mode for  $\Lambda = 1 \mu\text{m}$  and  $d/\Lambda = 0.5$  at  $\lambda = 1 \mu\text{m}$  (a) x-component of the electric field and (b) y-component of the electric field

and the total number of time steps  $2^{15}$ , the space increment is assumed to be  $\Delta h = \Lambda/134$ .

Letting  $n_{\text{silica}} = 1.450417$  (the refractive index for the fused silica at  $\lambda = 1 \mu\text{m}$  obtained from Sellmeier formula), the obtained numerical analysis indicates that the effective cladding index at  $\lambda = 1 \mu\text{m}$  is  $n_{\text{FSM}} = \beta_z/\beta = 1.43046$  ( $\beta$  is obtained by simulation), while the effective index obtained by FEM is 1.42994 (Brechet *et al.*, 2000). In another verification, by letting  $n_{\text{silica}} = 1.44402$  and calculating the effective cladding index at  $\lambda = 1.55 \mu\text{m}$ , the calculation results  $n_{\text{FSM}} = 1.40808$ , while the effective index obtained by FEM is 1.40836 (Brechet *et al.*, 2000). The (absolute) effective indices differences between the effective cladding indices obtained by the proposed method and those obtained by FEM are equal to or less than  $5.2 \times 10^{-4}$  and  $2.8 \times 10^{-7}$  at  $\lambda = 1$  and  $1.55 \mu\text{m}$ , respectively.

Figure 3a and b shows the patterns of the x- and y-components of the electric field of the fundamental mode for  $\lambda = 1 \mu\text{m}$ ,  $\Lambda = 1 \mu\text{m}$  and  $d/\Lambda = 0.5$ .

**RESULTS AND DISCUSSION**

Assuming  $n_{\text{silica}} = 1.45$  for all wavelengths,  $\Lambda = 1 \mu\text{m}$  and  $d/\Lambda = 0.4, 0.6$  and  $0.8$ , the cladding effective indices obtained by FDTD and FEM (Saitoh and Koshiba, 2005) are shown in Fig. 4.

Figure 4 shows that as  $d/\Lambda$  increases, the effective cladding index obtained by the proposed method deviates from the results by FEM. This difference is due to accuracy of FDTD algorithm, so that if the accuracy of the algorithm is improved, the deviation will decrease. For example the effective cladding index by FEM at  $\lambda/\Lambda = 1.0$  and  $d/\Lambda = 0.8$  is 1.23119, while by the proposed method for  $\Delta h = \Lambda/134$  and  $\Lambda/200$ , it is 1.22526 and 1.22827, respectively. Using Conformal technique is an alternative way to improve the accuracy, so by using averaged values of the constitutive parameters (Dey and Mittra, 1999), which has been earlier used in different methods, it is possible to improve the result. Using this technique, the effective cladding index for  $\Delta h = \Lambda/40$  is 1.23010 which is definitely better than the previous results. Therefore, the following results in the paper are calculated by using this method.

To investigate the advantage of using Padé approximation technique, the effective cladding index for  $\Lambda = 1 \mu\text{m}$  and  $d/\Lambda = 0.6$  is calculated. Figure 5 shows the merit of Padé approximation technique by comparing the results obtained by FFT and FFT/Padé.

Not only can Padé approximation technique improve the accuracy but also it is able to reduce the total number of time steps. To prove it,  $n_{\text{FSM}}$  at  $\lambda = 1 \mu\text{m}$  for total number

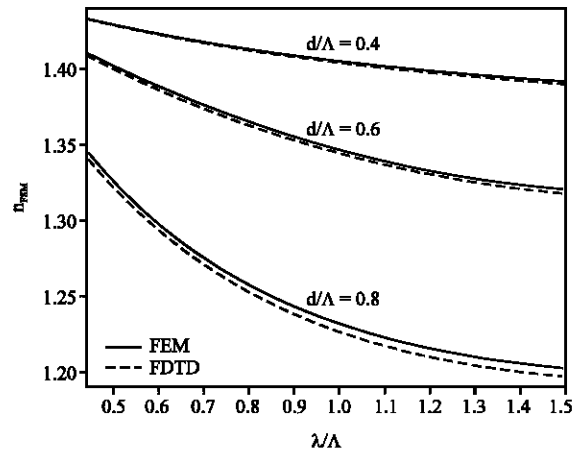


Fig. 4: The effective cladding index obtained by FDTD and FEM for  $\Lambda = 1 \mu\text{m}$  and  $d/\Lambda = 0.4, 0.6$  and  $0.8$

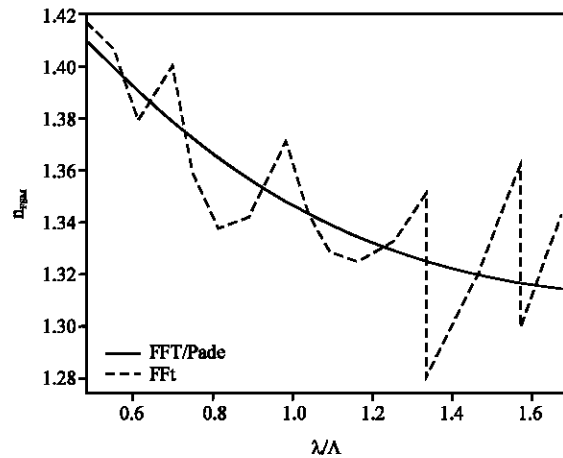


Fig. 5: Comparison of FFT and FFT/Padé results for the effective cladding index of a PCF for  $d/\Lambda = 0.6$

of time steps  $2^{16}$ , space increment of  $\Delta h = \Lambda/134$ ,  $d = 1 \mu\text{m}$  and  $\Lambda = 2.3 \mu\text{m}$  is calculated. The obtained numerical analysis indicates the effective cladding index without using FFT/Padé is 1.43326 which is quite deviated from the result of 1.42994 obtained by the FEM, While the result obtained by using FFT/Padé ( $n_{\text{FSM}} = 1.43046$ ) is in good agreement with that by FEM.

Based on EI methods, once having effective cladding index, it is possible to solve the characteristic equation of the step-index fiber to obtain effective index (Li *et al.*, 2004, 2006; Knight *et al.*, 1998). To demonstrate the accuracy of this method, the results of EIM which uses the proposed FSM solver with those of FDTD method which analyzes a PCF structure are compared. Following the procedure introduced in (Qiu, 2001), the effective index of mentioned PCF is calculated, while taking the time increment,

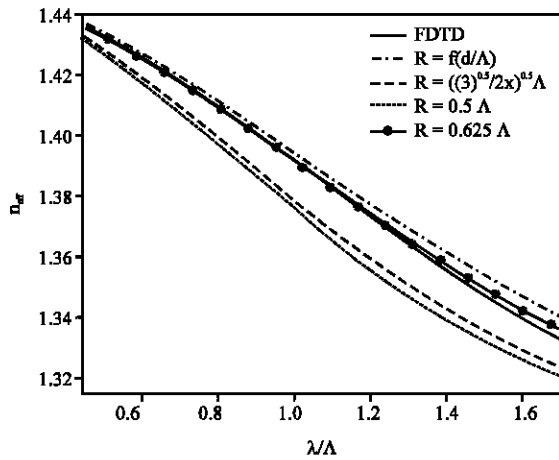


Fig. 6: Comparison of different effective radius results for the effective index of a PCF for  $\Lambda = 1 \mu\text{m}$  and  $d/\Lambda = 0.6$

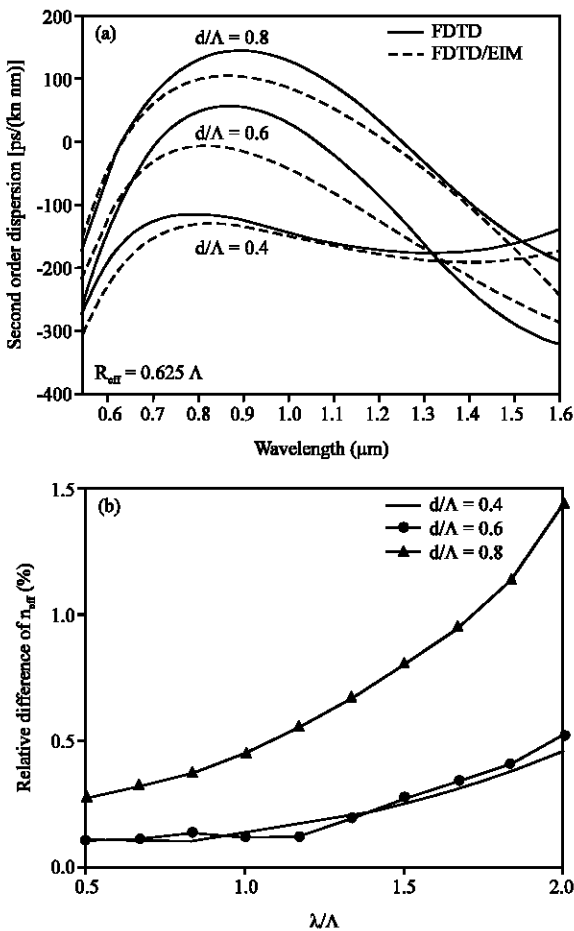


Fig. 7: Results obtained by FDTD and FDTD-EIM methods for  $\Lambda = 1 \mu\text{m}$  and  $d/\Lambda = 0.4, 0.6$  and  $0.8$ , (a) dispersion curves and (b) relative difference of  $n_{\text{eff}}$

$$\Delta t = 0.1/c\sqrt{2\Delta h^{-2} + \beta_z^2}/4$$

total number of time steps  $2^{15}$  and space increment  $\Delta h = \Lambda/20$ . Using the Convolutional Perfectly Matched Layer (CPML) technique (Roden and Gedney, 2000) for the FDTD boundary treatment, the excitation is done by initial field distribution and the results are obtained by FFT/Padé.

When using EI methods, the effective radius of the equivalent step index fiber can significantly change the result. It is found out that among common radii (Yong-Zhao *et al.*, 2006; Li *et al.*, 2004, 2006) used in various EIMs, leads to more accurate results. Figure 6 obviously proves this claim.

Furthermore, to study the accuracy of the solution on FDTD-EIM, the chromatic dispersion of a PCF by FDTD and FDTD-EI methods is calculated (Fig. 7).

According to Fig. 7, it is obvious that FDTD-EIM obtains less accurate results than FDTD method and one can see that for small  $d/\Lambda$ , the two methods obtain almost close results, so it is clear that although calculation of  $n_{\text{eff}}$  by solving the characteristic equation of the step-index fiber with  $R = 0.625 \Lambda$  leads to the best results compared with other proposed models with other common radii, it is not accurate enough to calculate the chromatic dispersion of PCF.

## CONCLUSION

In this study, by incorporating a specific periodic boundary condition for compact-2-D FDTD method, a method to solve the fundamental space-filling mode of a PCF could be presented. In order to increase the accuracy of analysis of results obtained by simulation, an initial field distribution which also could reduce the total number of time steps needed to reach steady state was proposed. A technique called Padé approximation was used to both decrease the total number of time steps and increase the accuracy of algorithm.

With the proposed FDTD fundamental space-filling mode solver, the effective cladding index of a typical PCF was numerically analyzed and the validity of the method was demonstrated. In addition, based on EI methods, the effective index by using different equivalent step-index fiber radii was calculated and it was shown that among common radii, the value of could lead to the best result nevertheless it could not lead to accurate results for the chromatic dispersion, therefore it is recommended to define a radius for equivalent step-index fiber so that the resulting error decreases as much as possible.

**REFERENCES**

- Asi, A. and L. Shafai, 1992. Dispersion analysis of anisotropic inhomogeneous waveguides using compact 2-D-FDTD. *Electron. Lett.*, 28: 1451-1452.
- Birks, T.A., J.C. Knight and P.S.J. Russell, 1997. Endlessly single-mode photonic crystal fiber. *Opt. Lett.*, 22: 961-963.
- Bjarklev, A., J. Broeng and A.S. Bjarklev, 2003. *Photonic Crystal Fibers*. Kluwer Academic Publisher, Boston, MA., ISBN: 1-4020-7610-X.
- Bowden, C.M. and A.M. Zheltikov, 2002. Nonlinear optics of photonic crystals. *J. Opt. Soc. Am. B*, 19: 2046-2048.
- Brechet, F., J. Marcou, D. Pagnoux and P. Roy, 2000. Complete analysis of the characteristics of propagation into photonic crystal fibers by the finite element method. *Opt. Fiber Technol.*, 6: 181-191.
- Choi, D.H. and W.J.R. Hoeffer, 1986. The finite-difference time-domain method and its application to eigenvalue problems. *IEEE Trans. Micro. Theory Techniques*, 34: 1464-1470.
- Dey, S. and R. Mittra, 1998. Efficient computation of resonant frequencies and quality factors of cavities via a combination of the finite-difference time-domain technique and the Padé approximation. *IEEE Micro. Guided Wave Lett.*, 8: 415-417.
- Dey, S. and R. Mittra, 1999. A conformal finite-difference time-domain technique for modeling cylindrical dielectric resonators. *IEEE Trans. Micro. Theory Techniques*, 47: 1717-1739.
- Ferrando, A., E. Silvestre, J.J. Miret, P. Andres and M.V. Andres, 1999. Full-vector analysis of a realistic photonic crystal fiber. *Opt. Lett.*, 24: 276-278.
- Hartl, I., X.D. Li, C. Chudoba, R.K. Rhanta and T.H. Ko *et al.*, 2001. Ultrahigh-resolution optical coherence tomography using continuum generation in an air-silica microstructure optical fiber. *Opt. Lett.*, 2: 608-610.
- Kliros, G.S., J. Konstantinidis and C. Thraskias, 2006. Prediction of macrobending and splice losses for photonic crystal fibers based on the effective index method. *WSEAS Trans. Commun.*, 5: 1314-1321.
- Knight, J.C., T.A. Birks, P.S.J. Russell and J.P. De-Sandro, 1998. Properties of photonic crystal fiber and the effective index model. *J. Opt. Soc. Am. A*, 15: 748-752.
- Konorov, S.O., D.A. Akimov, E.E. Serebryannikov, A.A. Ivanov, M.V. Alfimov and A.M. Zheltikov, 2004. Cross-correlation frequency-resolved optical gating coherent anti-Stokes Raman scattering with frequency-converting photonic-crystal fibers. *Phys. Rev. E*, 70: 057601-057604.
- Koshiba, M. and K. Saitoh, 2005. Simple evaluation of confinement losses in holey fibers. *Opt. Commun.*, 253: 95-98.
- Li, Y., C. Wang and M. Hu, 2004. A fully vectorial effective index method for photonic crystal fibers: Application to dispersion calculation. *Opt. Commun.*, 238: 29-33.
- Li, Y., C. Wang, Y. Chen, M. Hu, B. Liu and L. Chai, 2006. Solution of the fundamental space filling mode of photonic crystal fibers: Numerical method versus analytical approaches. *Applied Phys. B: Lasers Opt.*, 85: 597-601.
- Myaing, M.T., J.Y. Ye, T.B. Norris, T. Thomas and J.R. Jr. Baker *et al.*, 2003. Enhanced two-photon biosensing with double-clad photonic crystal fibers. *Opt. Lett.*, 28: 1224-1226.
- Nielsen, M., N. Mortensen, M. Albertsen, J. Folkenberg, A. Bjarklev and D. Bonacinni, 2004. Predicting macrobending loss for large-mode area photonic crystal fibers. *Opt. Express*, 12: 1775-1779.
- Paulsen, H.N., K.M. Hilligse, J. Thøgersen, S.R. Keiding and J.J. Larsen, 2003. Coherent anti-Stokes Raman scattering microscopy with a photonic crystal fiber based light source. *Opt. Lett.*, 28: 1123-1125.
- Qiu, M., 2001. Analysis of guided modes in photonic crystal fibers using the finite-difference time-domain method. *Microw. Opt. Tech. Lett.*, 30: 327-330.
- Qui, M. and S. He, 2000. Numerical method for computing defect modes in two-dimensional photonic crystals with dielectric or metallic inclusions. *Condensed Matter Mater. Phys.*, 61: 12871-12876.
- Ranka, J.K., R.S. Windeler and A.J. Stentz, 2000. Visible continuum generation in air-silica microstructure optical fibers with anomalous dispersion at 800 nm. *Opt. Lett.*, 25: 25-27.
- Reeves, W.H., D.V. Skryabin, F. Biancalana, J.C. Knight, P.S.J. Russell *et al.*, 2003. Transformation and control of ultra-short pulses in dispersion-engineered photonic crystal fibres. *Nature*, 424: 511-515.
- Roden, J.A. and S.D. Gedney, 2000. Convolutional PML (CPML): An efficient FDTD implementation of the CFS-PML for arbitrary media. *Microw. Opt. Technol. Lett.*, 27: 334-339.
- Saitoh, K. and M. Koshiba, 2005. Empirical relations for simple design of photonic crystal fibers. *Opt. Express*, 13: 267-274.
- Taflove, A. and S.C. Hagness, 2005. *Computational Electrodynamics: The Finite-difference Time-domain Method*. 3rd Edn., Artech House Publisher, Norwood, MA., ISBN: 1-58053-832-0.

- Udem, T., R. Holzwarth and T.W. Hänsch, 2002. Optical frequency metrology. *Nature*, 416: 233-237.
- Yee, K.S., 1966. Numerical solution of initial boundary value problems involving Maxwell's equations in isotropic media. *IEEE Trans. Antennas Propag.*, 14: 302-307.
- Yong-Zhao, X., R. Xia-Min, Z. Xia and H. Yong-Qing, 2006. A fully vectorial effective index method for accurate dispersion calculation of photonic crystal fibers. *Chin. Phys. Lett.*, 23: 2476-2479.
- Zhu, Z. and T. G. Brown, 2002. Full-vectorial finite-difference analysis of microstructured optical fibers. *Opt. Express*, 10: 853-864.